

Cold Energy Utilization by Stirling Engine

Krzysztof WIŚNIEWSKI¹ and Andrzej GRZEBIELEC*¹

¹Warsaw University of Technology, Warsaw, Poland

Abstract

Liquefied natural gas (LNG) will play an important role in the World, as evidenced by the constantly growing LNG market. One of its branches is the small-scale LNG market, which includes supplies to satellite gas networks, factories, or as fuel for car and bunker, fuel for vessels. LNG is mainly redistributed by trucks and then regassified in atmospheric air vaporizes (AAV), where the gas is heated by atmospheric air and the cold is thereby lost. Effective utilization of this energy, will allow the LNG technology to be more competitive, as well as to recover some of the energy lost in the liquefaction process. The purpose of this article is to explore the possibility of utilizing the cold energy from the LNG regasification process to drive a Stirling engine. For the aim of this analysis, an analytical method were used - Schmidt analysis, which assumes an isothermal processes of gas expansion and compression inside the engine, as well as excellent regenerator performance. Helium was used as a working factor. It was assumed, that the engine was arranged in accordance with alpha geometry. Average monthly air temperatures and average hourly temperatures for the coldest and warmest day of the year were applied to the model using macros and Excel worksheets. Those temperatures are the average from many years for Warsaw. Based on the applied data, the amount of regassified LNG, power of the entire system, indicated engine power, engine and system efficiency, as well as temperature in cylinders (and thus in heat exchangers) were calculated. The results showed the reasonability of using LNG as the lower heat source, and atmospheric air as the upper heat source. The system generates sufficient power, in all conditions, to meet the system energy consumption requirements i.e. fan. It produces significant excess amount of energy, which varies on the external conditions, i.e. the air temperature. In addition, the system meets the requirements for regassified amount of LNG at the end user.

Keywords: cryogenics, cold energy, Stirling engine.

1 Introduction

1.1 The Future of the Natural Gas

The natural gas is nowadays considered as one of the key fossil fuels. According to International Energy Agency (IEA) analysis, natural gas will be the key component in the transition process between conventional and new, effective and innovative power generation technologies. In Outlook for Natural gas 2018 [20] the IEA forecasts, that the Gas consumption will be rising in the next 20 years, regardless of the all environmental concern. It was concluded by the analysis of the 3 scenarios of the gas sector development: Current Policies Scenario, New Policies Scenario, and Sustainable Development Scenario. The Figure 1 shows the predicted gas consumption till 2040.

The consumption rising of the natural gas will be caused mostly by rising demand in Countries like China and India. It will also be influenced by the new unconventional sources of the natural gas, like the shell gas. The last 10 years had shown, that such unconventional resources can dramatically influence the global market of natural gas and the international energy policy. US is the best example. It has switched from the largest consumer in the world, to the one of the largest exporter of LNG.

The growing LNG market will also improve the natural gas consumption, because of the better availability of Natural Gas on the market. The LNG market is constantly developing [22] – in year 2019 the LNG global demand has increased about 13% comparing to 2018. It has reached 354,7 MT of LNG imported, and 34% of it was imported on the SPOT term basis (it is about 119 MT). About 69% of the global LNG demand is in Asia, especially in Japan, China, and India. In 2017 there were 42 importin Countries and 21 exporting. There are in total 920 MTPA capacity

*Corresponding author: E-mail address: andrzej.grzebielec@pw.edu.pl (Andrzej GRZEBIELEC)

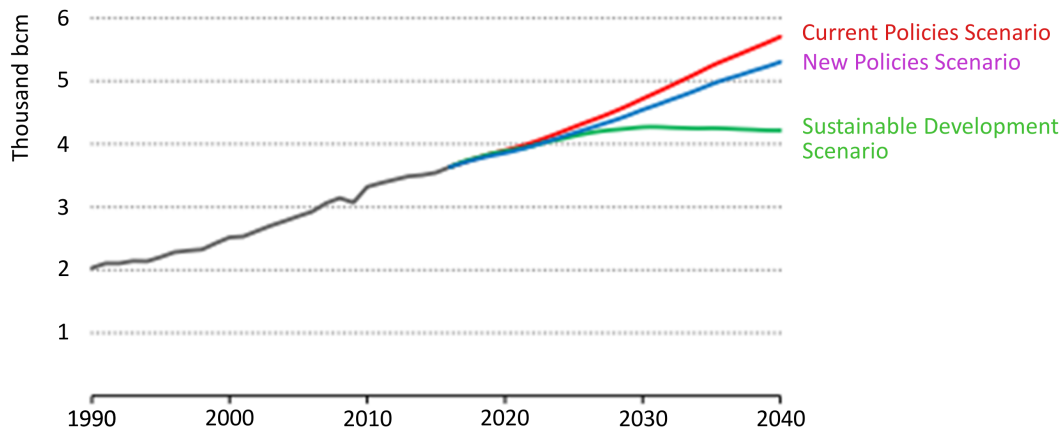


Figure 1. Gas consumption forecast till 2040 in billion cubic meters (bcm) [20]

of LNG regasification, and 427 MTPA of the NG liquefaction, in total. The LNG was transported by the fleet of 601 LNG carriers. Most of ships has less than 10 years of operation. The LNG covers almost 10% of the natural gas consumed in the World [11, 20, 22, 25]. Regasification process of LNG can also be used in processes such: seawater desalination, air compounds separation, natural gas purification, direct expansion or OTEC systems[2, 6–8, 15].

1.2 Influence of the LNG on Natural Gas Market

The LNG is an acronym of the liquefied natural gas [17]. Such state is achieved after cooling down the natural gas to the cryogenic temperature – usually it is about $-161\text{ }^{\circ}\text{C}$ (under normal condition) – to its liquid form, which takes about 600 times less volume than gaseous state [3]. Such condition gives possibility to transport NG without using gas pipelines, so it can reach areas, where the pipelines cannot reach for any reason. As a result, it opens the new possibilities of the natural gas market. For the largest natural gas consumers like Japan, China or India, LNG is the main way to import this resource.

The LNG, by definition, should consist of at least 87% of methane [3]. The rest of the composition consists of heavier hydrocarbons, mostly ethane and propane, sometimes some amount of nitrogen as well. In general the composition depends on the origin, what is showed in the Table 1 Quick look at the composition shows, that it is the most clean type of fossil fuel.

1.3 LNG supply chain

The LNG supply chain is divided into three segments; upstream, midstream, and downstream which are presented in Figure 2.



Figure 2. The supply chain of the LNG [5]

The upstream segment includes exploration and production (mining) natural gas. The midstream include production of the LNG in liquefaction plants and transport by large LNG carriers to the import terminals. This segment is also called large scale LNG segment. Downstream branch contain storage of LNG, regassification and further redistribution of the LNG from terminal by trucks, railways, iso containers or small vessels. The market around the

Table 1. The LNG composition by place of origin (from [9])

Origin	Nitro-gen N ₂ %	Methane C1%	Ethane C2%	Pro-pane C3%	C4+%	Total	LNG Density kg/m ³	Gas Density kg/m ³ (n)	Expan-sion ratio m ³ (n)/m ³ liq	Gas GCV MJ/mm ³ (n)	Wobbe Index MJ/m ³
Australia-NWS	0.04	87.33	8.33	3.33	0.97	100	467.35	0.83	562.46	45.32	56.53
Australia-Darwin	0.10	87.64	9.97	1.96	0.33	100	461.05	0.81	567.73	44.39	56.01
Algeria-Skikda	0.63	91.40	7.35	0.57	0.05	100	446.65	0.78	575.95	42.30	54.62
Algeria-Bethioua	0.64	89.55	8.20	1.30	0.31	100	454.50	0.80	571.70	43.22	55.12
Algeria-Arzew	0.71	88.93	8.42	1.59	0.37	100	457.10	0.80	570.37	43.48	55.23
Brunei	0.04	90.12	5.34	3.02	1.48	100	461.63	0.82	564.48	44.68	56.18
Egypt-Idku	0.02	95.31	3.58	0.74	0.34	100	437.38	0.76	578.47	41.76	54.61
Egypt-Damietta	0.02	97.25	2.49	0.12	0.12	100	429.35	0.74	582.24	40.87	54.12
Equatorial Guinea	0.00	93.41	6.52	0.07	0	100	439.64	0.76	578.85	41.95	54.73
Indonesia-Arun	0.08	91.86	5.66	1.60	0.79	100	450.96	0.79	571.49	43.29	55.42
Indonesia-Badak	0.01	90.14	5.46	2.98	1.40	100	461.07	0.82	564.89	44.63	56.17
Indonesia-Tangguh	0.13	96.91	2.37	0.44	0.15	100	431.22	0.74	581.47	41.00	54.14
Libya	0.59	82.57	12.62	3.56	0.65	100	478.72	0.86	558.08	46.24	56.77
Malaysia	0.14	91.69	4.64	2.60	0.93	100	454.19	0.80	569.15	43.67	55.59
Nigeria	0.03	91.70	5.52	2.17	0.58	100	451.66	0.79	571.14	43.41	55.50
Norway	0.46	92.03	5.75	1.31	0.45	100	448.39	0.78	573.75	42.69	54.91
Oman	0.20	90.68	5.75	2.12	1.24	100	457.27	0.81	567.76	43.99	55.73
Peru	0.57	89.07	10.26	0.10	0.01	100	451.80	0.79	574.30	42.90	55.00
Qatar	0.27	90.91	6.43	1.66	0.74	100	453.46	0.79	570.68	43.43	55.40
Russia-Sakhalin	0.07	92.53	4.47	1.97	0.95	100	450.67	0.79	571.05	43.30	55.43
Trinidad	0.01	96.78	2.78	0.37	0.06	100	431.03	0.74	581.77	41.05	54.23
USA-Alaska	0.17	99.71	0.09	0.03	0.01	100	421.39	0.72	585.75	39.91	53.51
Yemen	0.02	93.17	5.93	0.77	0.12	100	442.42	0.77	576.90	42.29	54.91

redistribution of the LNG to satellite regasification plant, LNG fuel stations, LNG fueled vessels, is called small scale LNG segment. This term is also related to the production in small liquefaction plants.

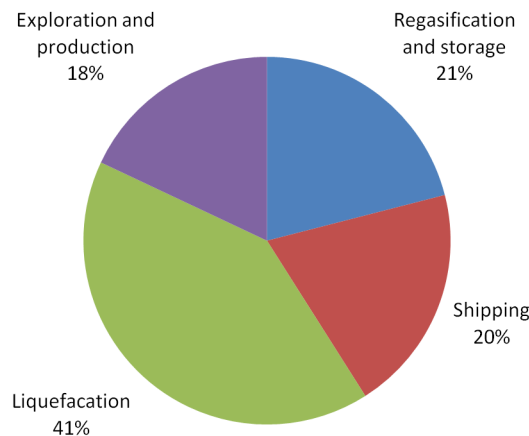


Figure 3. Cost breakdown of the LNG value chain [1]

The LNG is more expensive than natural gas. It is caused by more complex value chain than natural gas. In the figure 4 it is showed, that only 18% is the exploration and production. The rest of value is generated by liquefaction process (41%), transport (20%), storage and regasification (both about 21%).

1.4 Stirling engine based on LNG cold utilization systems

Almost all presented technologies of LNG cold utilization require to be in the near location to the LNG import terminal. What makes proposed solutions not suitable for small scale branch. However, it is not a case for Stirling engine, which is not limited in case of location. There are several publications related to Stirling engine driven with cryogenic energy and all of them are theoretical. Due to low temperature of LNG, there can be high gradient of temperatures, even with relatively low temperature of the heat source, what is crucial for Stirling Engine. The LNG in such system is used as a heat sink. The heat source can be selected according to the requirements and possibilities, but usually it is ambient air, waste heat or sea water.

Oshima et al. [18] in 1978 investigated combined regasification system with stirling power generation. The results show, that such system can be economically and functionality (LNG regassification) feasible. However, the main problem indicated by the author was the scale of the engine. There are no companies, which construct so large Stirling engines. Currently, it can be meet just RC cryogenics power generation systems (like in Osaka, Japan) [16, 19].

Szargut at al. [21] has proposed cryogenic Stirling cycle, which were driven by the “cold energy of the LNG”. The cycle is shown in the Figure 4.

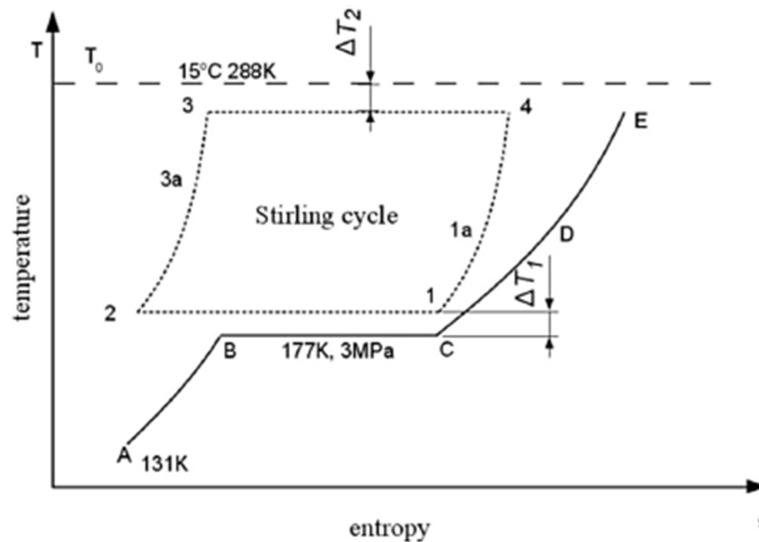


Figure 4. The proposed Stirling cryogenic cycle [21]

The research investigates the influence of the upper ΔT_2 and lower temperature ΔT_1 pinch, size of the dead volumes, and engine pressure compression on the exergy efficiency. It occurs, that the most important influence of the exergy efficiency has the dead volume capacity – with the increase of volume there were significant drop of exergy. On the other hand, the temperature pinch had limited effect on exergy efficiency. Moreover, the pressure ratio, according to their results, should be high, when its regenerator efficiency is poor.

Baris Burak Kanbur et al. [14] investigate the cogeneration system which has combined the Stirling Engine with micro gas turbine. It was compared with corresponding conventional system. Both systems were compared for wide range of ambient temperature and different compression ratio. In general, the increase in generated power was observed. The thermal efficiency was increased to about 1% and the exergy efficiency about 2,4%. The emissions reduction varies from 3,9% to 8%, depending on the pressure ratios.

Kai Wang et al. [23] investigate numerical analysis of the thermoacoustic Stirling. The system used simultaneously the waste heat and LNG cold energy. As a result, the cycle operated between temperatures 110 K and 500K. For assumed 4 MPa, absolute pressure inside the power output was at the level of 2,3 kW of electrical energy.

Although there is a lot of publications about the LNG cold energy utilization [13], there is few publications, which cover topic of Stirling engine driven by cold energy from re-harvesting cold energy [4]. Probably one of the reasons are the technical problems, and limitations of the Stirling engine which are still unsolved.

2 System Introduction

The analyzed system combines LNG vaporizer with Stirling Engine. The vaporizer is in the same time engine's cooler, so in fact the LNG works as a heat sink. The heat is delivered by the ambient air through the force convection. The whole system is showed in the Figure 5).

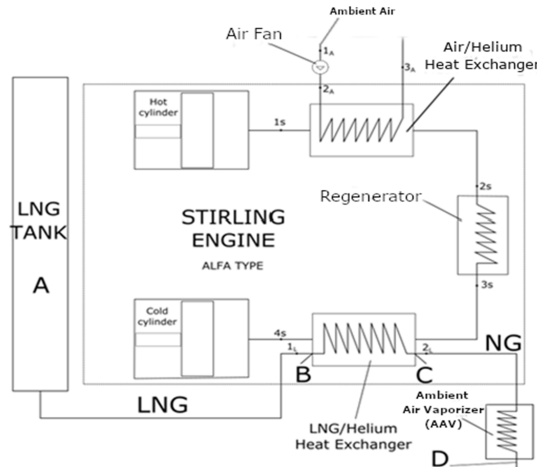


Figure 5. General view of the system

The model consists 4 elements: Stirling engine, Cooler, Heater and Fan.

2.1 Elements of the system

2.1.1 The LNG tank (point A)

The LNG tanks can store about 40 – 70 m³ of LNG. The number of tanks in the satellite station strictly dependent on the gas consumption of the end user. The LNG is stored under pressure between 1 – 7 bar, but it depends on storage time, weather conditions, and the pressured inside the trailer which delivered such cargo.

The LNG tank (point A in Figure 5 and Figure 6) is not directly included in the analysis. It is assumed, that the amount of stored LNG is large enough to maintain the steady flow. The absolute pressure assumed to be constant and is equal to 3 bars. This system does not require cryogenic pump to unload the tank – the LNG is pushed out by the weight of the LNG (the tank is oriented vertically).

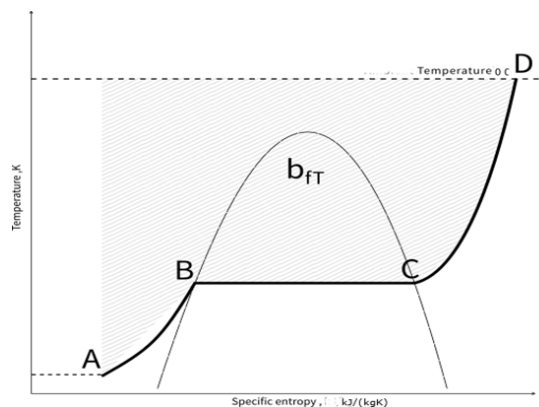


Figure 6. Temperature vs. entropy graph for LNG inside vaporizer

2.1.2 The Vaporizer (point B – C)

After the LNG is pushed out of the tank, it flows into the vaporizer (line B – C in Figure 6). In Figure 5 it is shown, that a vaporizer is in the same time also the Stirling engine cooler. In the Figure 6 the thermodynamic process is

showed. The pressure is assumed to be constant through the whole process. Additionally, the phase change from liquid natural gas to its gaseous form takes place at the end of regassificator. It means that there is only one phase on the shell side of vaporizer.

The LNG regassification and natural gas heating up process will be the same, as it was described in Szargut et al. [21] – see Figure 5 and Figure 6. The regassification process is assumed to be isobaric. The model is represented by line B-C.

3 Algorithm and methodology

3.1 Calculating the design point

First of all, the design point of the system is calculated for Schmidt analysis, using the formulas described in this chapter and applying excel macro, which enables to find point where all constrains are fulfilled. Additionally to the Schmidt analysis the following assumptions are taken into account:

- the nominal consumption of the natural gas by the end user is 1MW (1 MWh during 1 hour);
- the absolute LNG pressure is equal to 3 bar;
- flow of LNG and air are fully developed (thermally and dynamically);
- the gross calorific value based on the mass is assumed to $15.25 \left[\frac{kWh}{kg} \right]$;
- the LNG and air flow occur in the steady state;
- The phase change from liquid natural gas to its vapour form take place at the end of regassificator. It means that there is only one phase on the LNG – shell side;
- the physical characteristics (including pressure and temperature) are constant through the whole volume of the LNG in heat exchanger;
- the density of the LNG and air is assumed to be constant;
- the LNG regassification and heating up process is isobaric.
- the fin efficiency is assumed to be 75%.
- the Helium were choose as a working medium;
- the atmospheric air is assumed to be dry;
- the efficiency of the electric power generation is assumed to 98%.

3.2 Stirling Engine

3.2.1 Geometry

The piston diameter, swept volume ratio, dead volume ratios, engine speed, and phase angle were pre-assumed. The other parameters were calculated according to the formulas 1-6. In Table 2 the geometry of the Stirling engine is presented.

3.2.2 Determination of the Geometry

Piston Stroke is assumed to be half the diameter of the bore:

$$H = 1/D \quad (1)$$

Swept Expansion Volume is:

$$V_{sweptexp} = \frac{\pi}{4} H \cdot D^2 \quad (2)$$

Swept Compression Volume is:

$$V_{swptcomp} = V_{swptexp} \cdot \nu \quad (3)$$

Regeneration volume is:

$$V_{reg} = Xr \cdot V_{swptexp} \quad (4)$$

Dead Volume of (expansion volume) Heater:

$$V_{deadexp} = Xde \cdot V_{swptexp} \quad (5)$$

Dead volume of the (compression volume) Cooler:

$$V_{deadcomp} = Xdc \cdot V_{swptexp} \quad (6)$$

Table 2. Geometry of the Stirling engine

Parametr	Symbol	Value	Unit
Piston Diameter	D	0.25	[m]
Piston stroke	H	0.13	[m]
Swept volume ratio	ν	1.00	[-]
Swept Volume Compression cylinder	$V_{swptcomp}$	0.01	[m ³]
Swept Volume Expansion cylinder	$V_{swptexp}$	0.01	[m ³]
Dead volume ratio (Regenerator volume)	Xr	50.0	[%]
Dead volume ratio (Compression volume)	Xdc	71.4	[%]
Dead volume ratio (Expansion volume)	Xde	142.2	[%]
Regenerator Volume	V_{reg}	0.0031	[m ³]
Dead Volume of Compression part (cooler)	$V_{deadcomp}$	0.0044	[m ³]
Dead Volume of Expansion part (heater)	$V_{deadexp}$	0.0087	[m ³]
Engine speed	n	50	[Hz]
Phase angle	dx	92	[deg]

3.2.3 Calculation of the temperatures

As it was mentioned the Helium was chosen as a working medium for Stirling engine. The temperature difference of heater and cooler, were assumed. In the cooler the difference is defined as difference between helium and LNG temperature (which is constant through the heat exchanger [12]). The temperature difference in heater is defined as a difference between outlet temperature of air flowing through heat exchanger and helium temperature [24]. The mean pressure was pre-assumed, and then estimated using back-solving problem approach. The special macro were designed to meet constrains of the system. The results of the equations 7 – 11 are presented in Table 3.

Temperature in cold cylinder:

$$T_{Hecold} = T_{LNG} - \Delta T_{cooler} \quad (7)$$

Temperature in hot cylinder:

$$T_{Hehot} = T_{airo} - \Delta T_{heater} \quad (8)$$

Temperature in the Regenerator:

$$T_r = \frac{T_{Hecold} + T_{Hehot}}{2} \quad (9)$$

Temperature ratio:

$$t = \frac{T_{Hecold}}{T_{Hehot}} \quad (10)$$

Individual Gas constant:

$$R = \frac{B}{M_o} \quad (11)$$

Table 3. Parameters of the working medium

Parametr	Symbo	Value		Unit
Working Medium inside engine			Helium	
Molar mass	Mo		4	$[\frac{kg}{kmol}]$
Universal Gas Constant	B		8314	$[\frac{J}{kmolK}]$
Individual Gas Constant	R		2 077	$[\frac{J}{kgK}]$
Mean pressure	p_{mean}		8 227 008.53	[Pa]
Temperature difference in cooler between the helium and the LNG	ΔT_{cooler}		10	[K]
Temperature difference in heater between helium and the outlet temperature of air	ΔT_{heater}		5	[K]
Temperature of the helium in the compression volume of engine	T_{Hecold}		-136.44	[°C]
Temperature of the helium in the expansion volume of engine	T_{Hehot}		-0.29	[°C]
Temperature ratio	t		0.50	
Temperature of Helium inside the regenerator of the Stirling engine	T_r		-68.36	[°C]

3.2.4 Calculation of Schmidt analysis constants

The Schmidt analysis proposed several constants, which simplify calculations [10]. All results from calculations are related to constant and mass results from equations 12-16 and are presents in Table 4.

"B" constant:

$$B = \sqrt{(t^2 + 2 \cdot t \cdot v \cdot \cos(dx) + v^2)} \quad (12)$$

"S" constant:

$$S = t + 2 \cdot t \cdot Xde + \left(\frac{(4 \cdot t \cdot Xr)}{(1+t)} \right) + v + 2 \cdot Xdc \quad (13)$$

"C" constant:

$$C = \frac{B}{S} \quad (14)$$

"a" constant:

$$a = \arctan\left(\frac{v \cdot \sin(dx)}{t + \cos(dx)}\right) \quad (15)$$

mass of working medium inside the engine:

$$m = p_{mean} \frac{V_{swptexp} \sqrt{(S^2 - B^2)}}{2 \cdot R \cdot T_{Hecold}} \quad (16)$$

Table 4. Constants of the Stirling engine

Parametr	Symbol	Value	Unit
B constant	B	1.10	[-]
S constant	S	5.02	[-]
C constant	C	0.22	[-]
a constant	a	0.02	[rad]
Mass of working medium inside engine	m	0.81	[kg]

3.2.5 Work, power and efficiency of the engine

All results from equations 17 – 24 and are presents in Table 5.

Heat transfer rejected through the cooler:

$$Q_{out} = \frac{p_{mean} \cdot V_{swptexp} \cdot \pi \cdot t \cdot C \cdot \sin(a)}{(1 + (1 - c^2))} \quad (17)$$

Heat transfer which need to be delivered through the heater:

$$Q_{in} = \frac{p_{mean} \cdot V_{swptexp} \cdot \pi \cdot C \cdot \sin(a)}{(1 + (1 - c^2))} \quad (18)$$

It can be concluded that:

$$Q_{out} = t \cdot Q_{in} \quad (19)$$

Indicated work of engine is then:

$$W_{ind} = Q_{in} - Q_{out} \quad (20)$$

Efficiency:

$$\eta = \frac{W_{ind}}{Q_{in}} \quad (21)$$

Heat rate released by engine through the cooler:

$$\dot{Q}_{out} = Q_{out} \cdot n \quad (22)$$

Heat rate absorbed by engine through the heater:

$$\dot{Q}_{in} = Q_{in} \cdot n \quad (23)$$

Indicated power of the engine:

$$P_{in} = W_{ind} \cdot n \quad (24)$$

Table 5. The indicated power, heat transfers, heat rates and efficiency for the proposed geometry

Parametr	Symbol	Value	Unit
Heat rate rejected from engine through cooler	\dot{Q}_{out}	-8 741.00	[W]
Heat rate absorbed by engine through cooler	\dot{Q}_{in}	8 227 008.53	[W]
Indicated Power	P_{ind}	8 704.97	[W]
Heat released through cooler during one cycle	Q_{out}	-174.82	[J]
Heat absorbed through the heater during one cycle	Q_{in}	348.92	[J]
Indicated Work during one cycle	W_{in}	174.10	[J]
Cycle efficiency	η	50.00	[%]

For a purpose of the drawing of the cycle, the equations 25 – 27 were applied. The instantaneous expansion volume is calculated according:

$$V_{instexp} = \frac{V_{swptexp}}{2} \cdot (1 - \cos(x)) + V_{deadexp} \quad (25)$$

The instantaneous compression volume is based on formula:

$$V_{instcomp} = \frac{V_{swptexp}}{2} \cdot (1 - \cos(x - dx)) + V_{deadcomp} \quad (26)$$

The instantaneous pressure is calculated according to:

$$p_{inst} = \frac{2 \cdot m \cdot R \cdot T_{Hecold}}{V_{swptexp} \cdot (S - B \cdot \cos(dx - a))} \quad (27)$$

The Schmidt Stirling cycle is illustrated in the Figure 7.

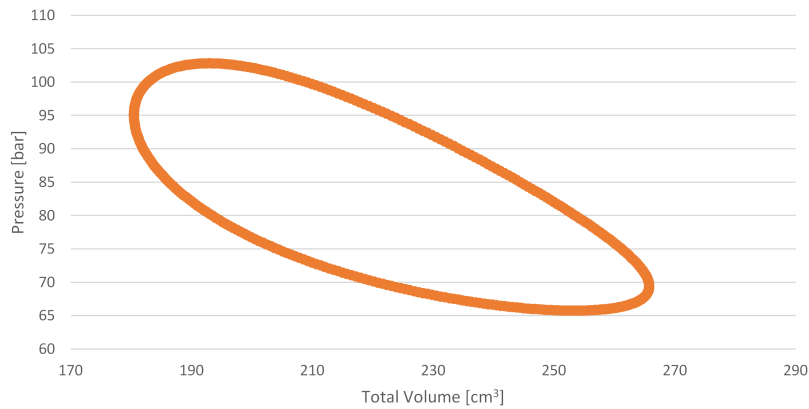


Figure 7. p-V diagram for calculated Stirling engine

The relation of the instantaneous expansion and compression volume to the phase angle of the engine are showed in Figure 8. The instantaneous volumes differ because of the dead volumes. It is caused by the size of heat exchangers. The pressure fluctuation inside the Stirling engine are presented in Figure 9. The calculation algorithm is presented in Figure 10.

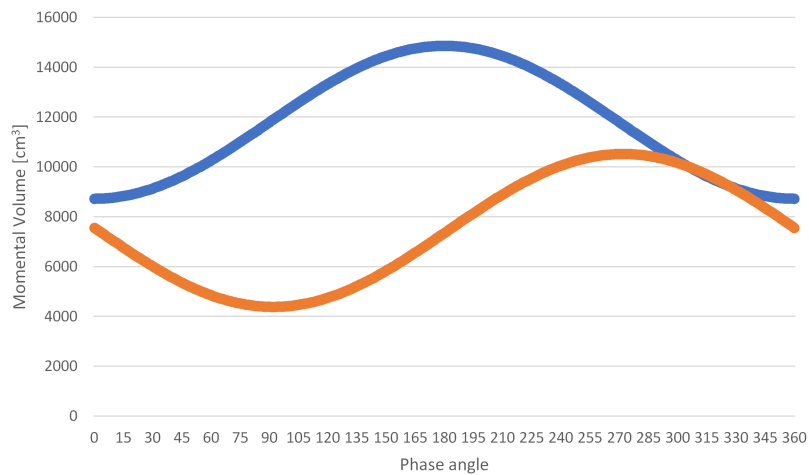


Figure 8. Instantaneous expansion and compression volume vs. phase angle of the Stirling engine

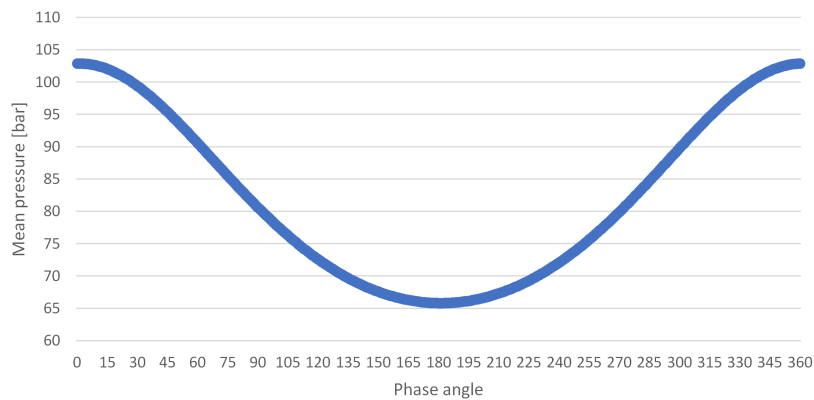


Figure 9. Instantaneous pressure vs. phase angle inside the engine

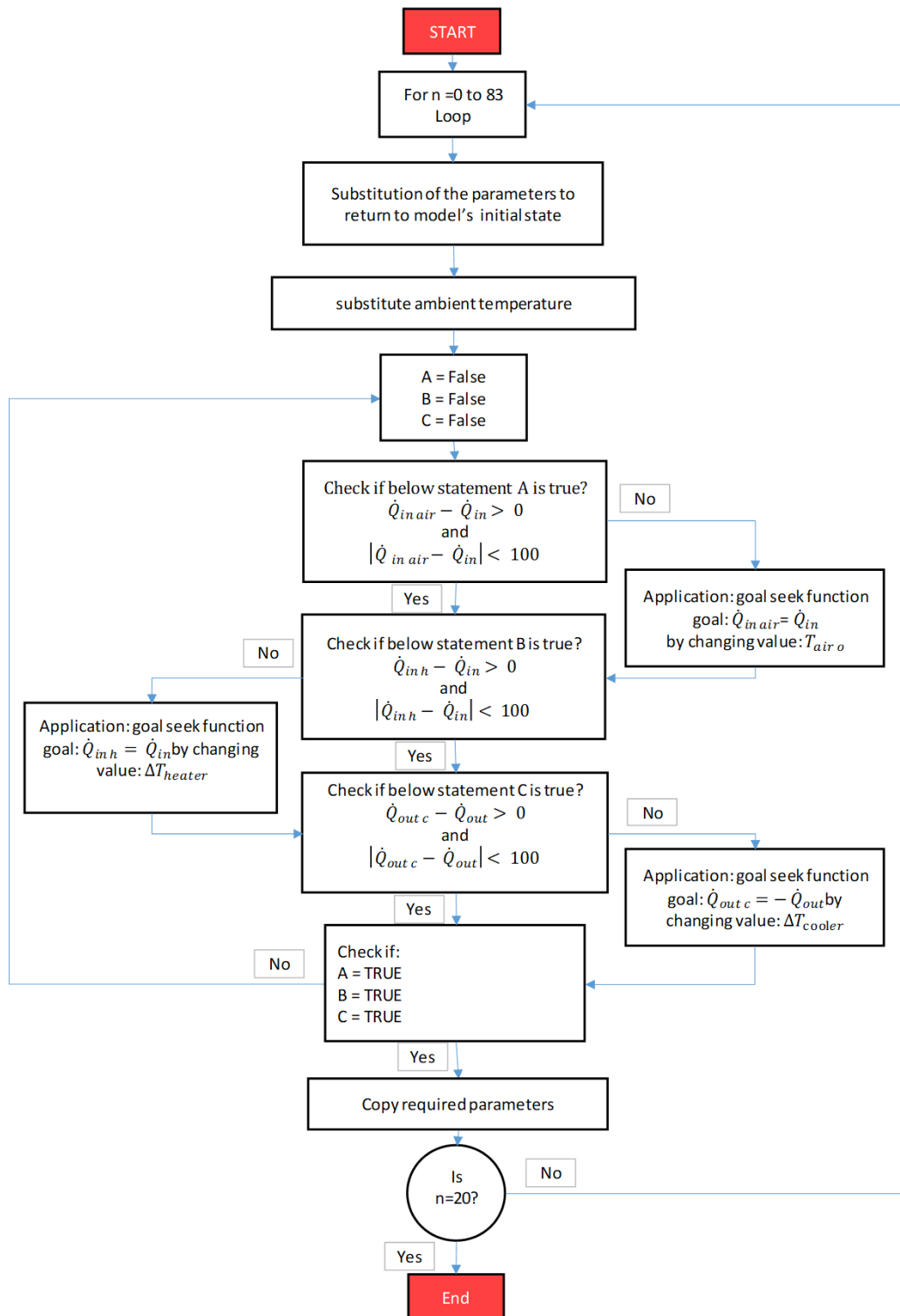


Figure 10. The algorithm used to generate result

3.3 Results

3.3.1 Temperature variation inside compression and expansion space in relation to average monthly daily temperature

The dependence between temperature inside compression and expansion space, to average monthly daily temperature are showed in Figure 11. Changes of the ambient temperature causes changes of temperate in expansion and com-

pression part of the engine. The lowest ambient temperature is -1.17°C and it is observed in January. It results with minimum temperature in expansion space, which is about -15.47°C and maximum in the compression space about -136.23°C . The highest mean daily temperature 19.18°C are observed in July. It results with maximum temperature in hot cylinder 3.60°C and minimum in the cold cylinder -136.44°C . The average temperature during year inside the expansion space is about -6.69°C . The temperature in compression piston and cooler is nearly stable and it differs only in tenth of Celsius degree. The mean temperature gap between heater (expansion space) and ambient air is about 14.88°C .

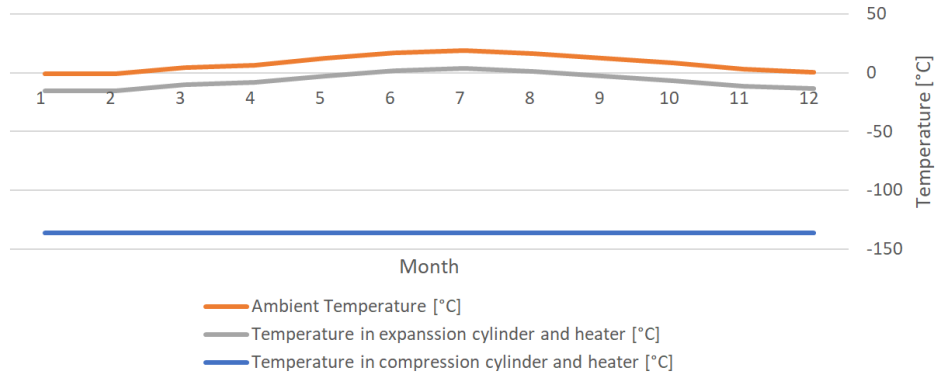


Figure 11. Temperature variation inside compression and expansion space in relation to daily average monthly temperature

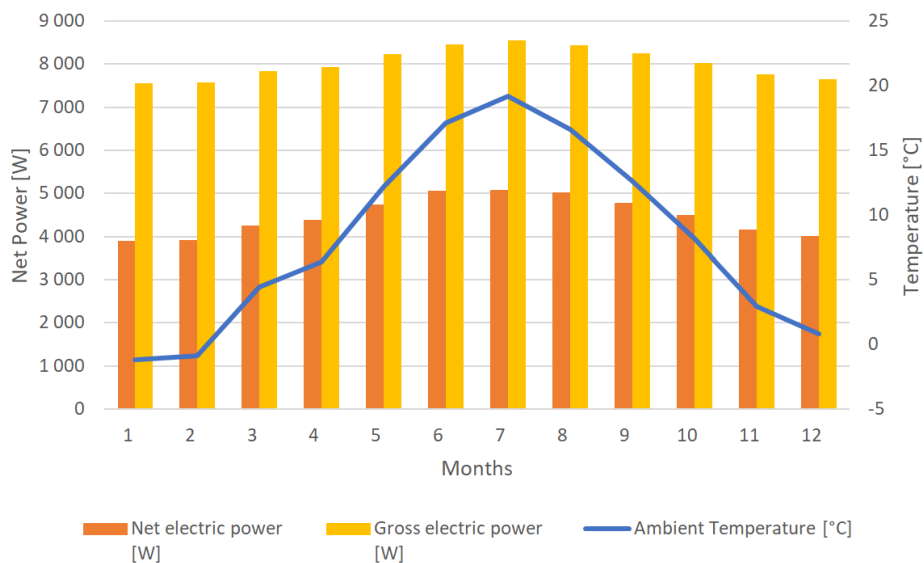


Figure 12. Net electric power generation output of the system in relation to daily average monthly temperature.

Net electric power generation of the system and generator, in relation to average monthly daily temperature is shown in Figure 12.

3.3.2 Efficiency of the engine and the system related to average monthly daily temperature

Efficiency of the engine and the system related to average monthly daily temperature are shown in Figure 13. For the highest ambient temperature 19.18°C in July, the efficiency reaches the highest value, which is 51%. Analogically, the efficiency drop to the lowest 47% in January, when there is the lowest temperature -1.17°C . The average efficiency of the engine is about 49%. When the electric power consumed by fan is included, the system efficiency drops to the average value 26%. Analogically to the engine efficiency, the highest value is achieved, when there is the highest ambient temperature in July, and it is 29%. The lowest efficiency is in January, and it is 23%.

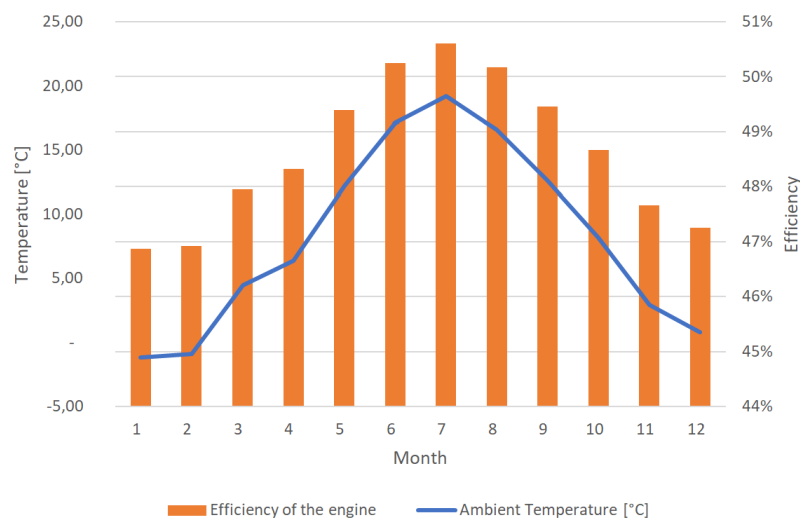


Figure 13. Efficiency of the engine and the system related to average monthly daily temperature

4 Conclusion

The general conclusion, based only on the results generated by the model, is that the proposed idea, system and geometry is reasonable and efficient. Due to large temperature difference between cold and hot cylinders, air can be successfully applied as a heat source. The system is capable to generate additional electric power from re-harvesting cold energy and the efficiency of the proposed engine is very high. The yearly average gross electric power of the engine is 8020.84 W, the net electric power is about 4482.84 W, after including the electric power required by the fan. In the worst scenario – during the coldest day of the year – it is about 6984.63 W and 3410.60 W of gross and net electric power respectively. For the best scenario – the warmest day the average gross and net electric power are respectively 8932.58 W and 5354.17 W. The yearly average efficiency of the engine is high and it is about 49% and it varies 47% to 51%, depending on the outside ambient temperature. The efficiency of the overall system is much smaller and it varies between 23% – 29% with average value 26%. The efficiency drops almost twice, which shows the sensitivity of the system for applying any fan or pump. It should be decreased by applying different type of the heat source, optimized or with more efficient fan.

The system is capable of maintaining proper level of the natural gas in terms of power at the end of the vaporizer – which is one of the main goal of such system. However, during the warmest day, the regassification rate maintain at the average level 0.9 MWh, so below assumed quantity (1 MWh). The difference is small and it can be acceptable – it can be compensate in some other way. Another important conclusion is that the output power is similar for day and night, so there is no limitation in case of time of application.

The Schmidt analysis has several approximation and due to that - it is highly idealized. It means that the real results can be quite different. First of all for speeds above 1000 RPM the compression and expansion processes are more adiabatic than isothermal – in analyzed case the RPM was 3000 RPM. The regeneration process is also assumed to be ideal, when in reality it can regenerate only part of heat what influence the temperature distribution in engine, and in the end it decreases the output power. Moreover, the size of regenerator was assumed – no calculations or analysis were performed for this part of engine – so it is not certain, if its volume is enough to provide proper operation. The model also exclude losses inside the engine. The main pressure losses results from the flow of the medium inside the heat exchanger channels and regenerator, loss through the sealing (which is a quite serious problem for Stirling engines) and internal losses of the medium due to vortex etc. It should be also marked, that the LNG regasification process was assumed to be isobaric. The helium is treated as an ideal gas, but around 80 – 100 bars, some correction should be taken into account. The other important remark is thermal efficiency. In Schmidt analysis efficiency is constant – it is not dependent on phase angle. However, in reality it varies upon the change of phase angle.

The Analysis has showed several challenges during designing process and pointed the direction of further developments and investigations. The main challenge was to desig proper heat exchanger. In general, there are two practices of designing such heat exchangers depending on the required heat load. First way is to attach fins to the wall of the cylinders, but it is not so efficient so it suits only to small engines. The other way is to use small channels derived

out of the engine, which gives a lot of possibilities to design such a system. However, it increases the dead volume and losses inside engine. So Heat exchanger need to fulfilled 3 opposing goals: it should transfer as much heat as it possible, cause minimum pressure losses and be compact, to minimize dead volume. For that reasons, it is crucial to choose proper heating fluid and type of heat exchanger. In analyzed case, the air is a heating medium and compact heat exchanger is applied as a heater. In case of cooler, the bundle of tubes submerged in the LNG flow. Although the compact heat exchanger was applied as a heater, it occupies significant volume of the engine, which is 0.0087 m^3 and it covers 142.2% of the swept volume. The cooler takes only 0.0044 m^3 , which covers 71.4% of the swept volume. The heater is over twice the coolers size. It is caused by different amount of heat, which needs to be transferred by them, but also different heating-cooling medium. To reduce those volumes, the other heating medium should be applied with sufficiently high specific heat. It can be concluded, that another medium should be investigate to improve system.

Another problem, is to design the proper size of the engine. Two factors must be taken into account: the proper mean pressure should be maintained inside engine and the velocity of medium inside the heat exchanger channels should not be too high. For bulkier engine, lower mean pressure of the working medium is required, but more channel need to be attached. It causes two problems: firstly, the problem with attaching the pipes to the cylinder, because there can be no enough space to attached all required pipes and secondly it increases pressure losses.

References

1. Al-Mutaz, I. S., Wazeer, I., Khan, R. & Chafidz, A. Process selection and recent design innovations for LNG plants - Part 1. *Gas Processing and LNG* (2019).
2. Arcuri, N., Bruno, R. & Bevilacqua, P. LNG as cold heat source in OTEC systems. *Ocean Engineering* **104**, 349–358. ISSN: 0029-8018 (2015).
3. Basic Properties of LNG. *GIIGNL Information Paper No 1* (2009).
4. Buliński, Z. *et al.* Finite time thermodynamic analysis of small alpha-type Stirling engine in non-ideal polytropic conditions for recovery of LNG cryogenic exergy. *Energy* **141**, 2559–2571. ISSN: 0360-5442 (2017).
5. Canepa, M. *Pricing on gas: focus on LNG sectors* (GoLNG, 2020).
6. Cao, W., Beggs, C. & Mujtaba, I. M. Theoretical approach of freeze seawater desalination on flake ice maker utilizing LNG cold energy. *Desalination* **355**, 22–32. ISSN: 0011-9164 (2015).
7. Franco, A. & Casarosa, C. Thermodynamic analysis of direct expansion configurations for electricity production by LNG cold energy recovery. *Applied Thermal Engineering* **78**, 649–657. ISSN: 1359-4311 (2015).
8. Gao, T., Lin, W. & Gu, A. Improved processes of light hydrocarbon separation from LNG with its cryogenic energy utilized. *Energy Conversion and Management* **52**. 9th International Conference on Sustainable Energy Technologies (SET 2010), 2401–2404. ISSN: 0196-8904 (2011).
9. *GIIGNL 2018 Annual Report* (International Group of Liquefied Natural Gas Importers, 2018).
10. Hirata, K. *Schmidt Theory for Stirling Engines* <http://www.bekkoame.ne.jp/~khirata/academic/schmidt/schmidt.htm> (2019).
11. Jiang, K. in *Energy Solutions to Combat Global Warming* (eds Zhang, X. & Dincer, I.) 119–132 (Springer International Publishing, Cham, 2017). ISBN: 978-3-319-26950-4.
12. Kakaç, S., Liu, H. & Pramuanjaroenkij, A. *Heat Exchangers. Selection, Rating, and Thermal Design* edition Third edition. ISBN: 9781466556164 (CRC Press, 2012).
13. Kanbur, B. B., Xiang, L., Dubey, S., Choo, F. H. & Duan, F. Cold utilization systems of LNG: A review. *Renewable and Sustainable Energy Reviews* **79**, 1171–1188. ISSN: 1364-0321 (2017).
14. Kanbur, B. B., Liming, X., Dubey, S., Hoong, C. F. & Duan, F. Dynamic exergetic and environmental assessments of the small scale LNG cold utilized micro power generation systems. *Energy Procedia* **143**, 680–685. ISSN: 1876-6102 (2017).
15. Mehrpooya, M., Kalhorzadeh, M. & Chahartaghi, M. Investigation of novel integrated air separation processes, cold energy recovery of liquefied natural gas and carbon dioxide power cycle. *Journal of Cleaner Production* **113**, 411–425. ISSN: 0959-6526 (2016).
16. Miyazaki, T, Kang, Y., Akisawa, A & Kashiwagi, T. A combined power cycle using refuse incineration and LNG cold energy. *Energy* **25**, 639–655. ISSN: 0360-5442 (2000).
17. *Handbook of Liquefied Natural Gas* (eds Mokhatab, S., Valappil, J. V., Mak, J. Y. & Wood, D. A.) (Gulf Professional Publishing, 2014).
18. Oshima, K., Ishizaki, Y., Kamiyama, S., Akiyama, M. & Okuda, M. The utilization of LH2 and LNG cold for generation of electric power by a cryogenic type stirling engine. *Cryogenics* **18**, 617–620. ISSN: 0011-2275 (1978).
19. Otsuka, T. *Evolution of an LNG Terminal: Senboku Terminal of Osaka Gas* in. 23rd World Gas Conference, Amsterdam 2006 (2006).

20. *Outlook for Natural Gas 2018* (International Energy Agency, 2018).
21. Szargut, J. & Szczygiel, I. Utilization of the cryogenic exergy of liquid natural gas (LNG) for the production of electricity. *Energy* **34**, 827–837. ISSN: 0360-5442 (2009).
22. *The LNG industry. GIIGNL Annual Report* (International Group of Liquefied Natural Gas Importers, 2020).
23. Wang, K., Dubey, S., Choo, F. H. & Duan, F. Thermoacoustic Stirling power generation from LNG cold energy and low-temperature waste heat. *Energy* **127**, 280–290. ISSN: 0360-5442 (2017).
24. Wiśniewski, S. *Wymiana Ciepła* (Wydawnictwo Naukowo-Techniczne, Warszawa, 2012).
25. *Ze Świnoujścia wyjechało już 4000 autocystern ze skroplonym gazem LNG* Polskie Górnictwo Naftowe i Gazownictwo S. A. <http://pgnig.pl/aktualnosci/-/news-list/id/ze-swinoujscia-wyjechalo-juz-4000-autocystern-ze-skroplonym-gazem-lng/newsGroupId/10184?changeYear=2019¤tPage=11> (2019).